https://doi.org/10.5194/egusphere-2026-877
Preprint. Discussion started: 22 June 2026

Global controls on aftershock productivity: roles of magnitude and tectonic setting

Antonino D'Alessandro
Istituto Nazionale di Geofisica e Vulcanologia, Osservatorio Nazionale Terremoti, Rome, Italy
antonino.dalessandro@ingv.it

Abstract

Aftershock productivity varies substantially among large earthquakes, yet the relative roles of magnitude, tectonic environment, and source properties remain incompletely resolved at the global scale. Here we perform a comprehensive, data-driven analysis of aftershock productivity for all Mw ≥ 7.0 mainshocks worldwide since 1976, using a homogeneous workflow based on USGS/NEIC catalogs, PB2002 plate-boundary geometries, and uniformly defined aftershock windows ($r \leq 200$ km, $t \leq 30$ days, $M \geq 4.5$). Mainshock events are classified into three tectonic domains—subduction, other plate boundaries, and intraplate/crustal—allowing systematic comparison of productivity patterns across geodynamic settings. Across all tectonic classes, aftershock productivity scales linearly with mainshock magnitude in log-space, with nearly identical slopes ($b \approx 0.76$–0.81), indicating a universal magnitude-controlled triggering mechanism. In contrast, intercepts differ significantly among tectonic environments: subduction earthquakes are systematically the most productive, followed by other plate-boundary events and intraplate earthquakes. Depth and distance to the nearest plate boundary exert weaker but physically interpretable secondary influences, with productivity decreasing for deeper ruptures and for intraplate events located far from plate boundaries. Residual analysis and multivariate correlations confirm that magnitude and tectonic setting explain the dominant share of global variability, whereas depth and distance provide secondary, context-dependent modulation. Together, these results establish the first unified,

https://doi.org/10.5194/egusphere-2026-877
Preprint. Discussion started: 22 June 2026

physically interpretable global framework of aftershock productivity, quantifying both universal magnitude-driven scaling and environment-specific productivity offsets. The findings provide actionable constraints for global ETAS parameterization, operational aftershock forecasting, and seismic-hazard models for future great earthquakes.

Keywords

Aftershock productivity, Earthquake triggering, Tectonic setting, Global seismicity, Mainshock–aftershock scaling, Seismic hazard forecasting.

Highlights

We quantify how earthquake magnitude and tectonic setting jointly control global aftershock productivity

Aftershock productivity scales universally with magnitude but shows systematic offsets among tectonic settings

These results improve global aftershock forecasting and inform tectonic-dependent seismic hazard models

https://doi.org/10.5194/egusphere-2026-877
Preprint. Discussion started: 22 June 2026

1. Introduction

Aftershock sequences represent a fundamental component of the short-term temporal evolution of seismicity following large earthquakes. Their spatiotemporal decay is commonly described by the modified Omori–Utsu law (Omori, 1894; Utsu, 1961; Utsu et al., 1995), whereas the absolute number of aftershocks, or aftershock productivity, is typically parameterized through empirical magnitude-dependent scaling relations (Reasenberg and Jones, 1994; Helmstetter and Sornette, 2003; Shcherbakov et al., 2004; van der Elst and Page, 2014). This scaling, in its simplest form, expresses the number of aftershocks above a threshold magnitude as an exponential function of the mainshock magnitude and controls key components of operational earthquake forecasting models, including ETAS (Epidemic-Type Aftershock Sequence) formulations (Ogata, 1998; Zhuang et al., 2004; Marzocchi and Lombardi, 2009; Omi et al., 2013; Hainzl, 2016).

Despite decades of regional and global studies, significant uncertainty remains regarding the physical and tectonic controls on aftershock productivity. Most previous analyses have been conducted at regional scales (e.g., California, Japan, New Zealand), where local rheology, faulting style, and catalog completeness strongly influence observed productivity patterns (Felzer et al., 2002; Helmstetter, 2003; Marsan and Lengliné, 2008; Nishimura et al., 2020). Global studies are comparatively fewer and often rely on heterogeneous datasets, merging catalogs of variable completeness and mixing different tectonic environments (Parsons, 2002; Page et al., 2016; van der Elst, 2021). As a result, quantifying global rules that robustly describe how aftershock productivity varies with earthquake magnitude and tectonic setting remains an open problem of high scientific and practical relevance.

Tectonic environment is known to influence earthquake rupture characteristics, stress drop, and fault zone rheology (Scholz, 2002; Kanamori and Brodsky, 2004; Lay and Kanamori, 2011). Subduction megathrusts, for example, exhibit large rupture dimensions, high slip velocities, and high heat production, potentially favoring more abundant aftershock sequences (Lay et al., 2005; Hayes et al., 2018). Conversely, intraplate earthquakes often nucleate within colder, stronger lithosphere and may

https://doi.org/10.5194/egusphere-2026-877
Preprint. Discussion started: 22 June 2026

exhibit lower background seismicity rates and different stress-transfer efficiency (Scholz, 2019; Craig et al., 2017). However, a systematic, quantitative comparison of aftershock productivity across tectonic environments at the global scale has been lacking, largely due to the absence of unified classification frameworks and globally homogeneous aftershock datasets.

An additional source of uncertainty concerns the role of factors other than magnitude and tectonic setting. Several studies have proposed possible dependencies of aftershock productivity on depth (Parsons, 2002; Uchide et al., 2013), rupture complexity (Nishimura et al., 2020), mainshock stress drop (Hainzl et al., 2016; van der Elst, 2021), or background seismicity rate (van der Elst and Page, 2014). Yet these effects are often difficult to isolate due to catalog incompleteness, regional variability, and the strong primary control of magnitude itself. Clarifying the extent to which secondary variables—such as mainshock depth or distance to plate boundary—affect aftershock productivity is essential for improving physical models of earthquake triggering and for establishing globally applicable scaling laws.

In this study, we address these open questions by constructing a unified global dataset of $M_w \geq 7$ mainshocks and their aftershocks ($M_w \geq 4.5$) from 1976 to 2024, using the USGS NEIC catalog, ensuring consistent magnitude reporting and near-global completeness above Mw 4.5. Each mainshock is assigned to a tectonic class (SUBDUCTION, OTHER PLATE-BOUNDARY, INTRAPLATE/CRUSTAL) using distances to PB2002 plate boundaries (Bird, 2003), enabling a systematic comparison of aftershock productivity across contrasting tectonic regimes. In this study, aftershock productivity is defined in an operational and observation-based sense, rather than as the total number of triggered events in a fully cascading epidemic-type aftershock sequence (ETAS) framework. This operational definition is intentionally adopted to enable consistent, global-scale comparisons across heterogeneous tectonic environments and catalog conditions. The fixed spatial ($r \leq 200$ km) and temporal ($t \leq 30$ days) windows are not intended to capture the full physical extent or duration of individual aftershock sequences, which are known to scale with mainshock magnitude and rupture dimensions. Rather, they provide a standardized observational metric that minimizes

https://doi.org/10.5194/egusphere-2026-877
Preprint. Discussion started: 22 June 2026

subjective sequence delineation and ensures reproducibility at the global scale. While this approach may truncate late or far-field aftershocks of the largest earthquakes and include limited background activity for smaller mainshocks, these effects act systematically across the dataset and primarily affect absolute counts rather than relative scaling. Consequently, the analysis focuses on comparative productivity trends and regression-based offsets among tectonic settings, rather than on absolute estimates of total aftershock numbers. Specifically, productivity is quantified as the number of earthquakes with Mw $\geq$ 4.5 occurring within a fixed spatiotemporal window following each mainshock. This definition is designed to ensure global consistency, reproducibility, and robustness across heterogeneous tectonic environments and catalog qualities. We quantify aftershock productivity through both absolute aftershock counts and the logarithmic scaling log10(N+1) as a function of magnitude, depth, and tectonic setting.

Our goals are threefold:

- to quantify robust global scaling relations between aftershock productivity and mainshock magnitude,
- to determine how aftershock productivity varies across the major tectonic regimes of the planet, and
- to assess whether secondary variables (mainshock depth, proximity to plate boundaries) significantly affect productivity once magnitude and tectonic class are accounted for.

By combining global-scale data, tectonic classification, regression analyses, and residual-based diagnostics, this work offers a comprehensive assessment of the controls governing aftershock productivity. The resulting framework highlights the dominant roles of magnitude and tectonic setting, while constraining the comparatively weaker effects of depth and distance from plate boundaries. These results have direct implications for global earthquake triggering models, seismic hazard assessment, and the parameterization of operational forecasting systems at regional and global scales.

https://doi.org/10.5194/egusphere-2026-877
Preprint. Discussion started: 22 June 2026

2. Data and Methods

We compiled a global catalog of large earthquakes from the USGS/NEIC ComCat database, selecting all events of moment magnitude Mw ≥ 7.0 that occurred between 1 January 1976 and 31 December 2024. This time period ensures compatibility with the modern global seismic network and provides uniform moment-magnitude estimates worldwide. The adopted aftershock magnitude threshold (Mw ≥ 4.5) lies safely above the global magnitude of completeness for teleseismically recorded earthquakes throughout the study period. Previous assessments of global catalogs indicate that events of this size are reliably detected worldwide since the mid-1970s, including oceanic and remote regions. As a result, the completeness of the aftershock catalog is not expected to vary significantly over time at the selected magnitude threshold. For each mainshock, we retained origin time, epicentral coordinates, depth, and magnitude, along with relevant event metadata.

To quantify aftershock productivity, we used the same catalog to extract all earthquakes with Mw ≥ 4.5 within a 200 km radius and 30-day time window after each mainshock. These thresholds reflect a balance between catalog completeness, consistency with prior global analyses, and robust detectability across decades of heterogeneous network coverage.

To assess catalog completeness and its temporal stability, we evaluated the magnitude of completeness (Mc) of the global earthquake catalog over the study period. Previous global analyses of the USGS/NEIC ComCat and ISC-GEM catalogs indicate that Mc for moment magnitude has been consistently below Mw 4.5 since the mid-1970s, with progressive improvements in detection capability over time primarily affecting smaller magnitudes. To further verify that temporal variations in network coverage do not bias our results, we repeated key analyses by subdividing the catalog into three partially overlapping time periods (1976–1990, 1991–2005, and 2006–2024).

Across all time windows, the Mw–aftershock productivity scaling and the relative offsets among tectonic classes remain stable within statistical uncertainty. This confirms that the adopted Mw ≥ 4.5

https://doi.org/10.5194/egusphere-2026-877
Preprint. Discussion started: 22 June 2026

threshold lies safely above Mc throughout the study period and that the observed productivity patterns are not artifacts of long-term improvements in global seismic monitoring.

We explicitly acknowledge that the use of a fixed spatial (200 km) and temporal (30 days) window does not fully capture the magnitude-dependent extent and duration of aftershock sequences. Large earthquakes (Mw ≥ 8) commonly generate aftershocks over fault lengths exceeding several hundred kilometers and over timescales of months to years, whereas smaller Mw 7 events typically exhibit more compact and shorter-lived sequences. As a result, the adopted window may include background seismicity for lower-magnitude mainshocks while partially truncating the aftershock sequences of the largest events. However, because the same spatiotemporal criteria are applied uniformly to all events, this approach provides a consistent, reproducible measure of *relative* aftershock productivity across tectonic settings. The objective of this study is not to estimate the absolute number of triggered earthquakes, but to quantify comparative productivity scaling and systematic offsets among tectonic domains under a common observational framework. Because the analysis focuses on relative productivity scaling and inter-class comparisons rather than absolute rates, potential long-term improvements in network sensitivity primarily affect background detection levels and do not alter the observed magnitude dependence or tectonic offsets. Any residual temporal variations are therefore expected to contribute only second-order noise to the analysis. Accordingly, the productivity measure adopted here should be interpreted as a standardized empirical proxy that captures relative triggering efficiency across earthquakes and tectonic environments, rather than as a direct estimate of ETAS branching ratios or background-independent triggering rates.

To evaluate the robustness of our results with respect to the adopted spatiotemporal window, we performed a sensitivity analysis using alternative search radii and time windows. Specifically, aftershock productivity was recomputed using combinations of spatial radii r = 100 km, 200 km, and 300 km, and temporal windows t = 7 days, 30 days, and 90 days. For each configuration, we repeated the magnitude–productivity regressions and compared the resulting slopes and intercepts across tectonic classes.

https://doi.org/10.5194/egusphere-2026-877
Preprint. Discussion started: 22 June 2026

The sensitivity tests show that while absolute productivity values vary with r and t, the key results of this study remain stable: (i) the Mw–productivity slope is nearly invariant across window choices, and (ii) systematic intercept differences between subduction, other plate-boundary, and intraplate earthquakes persist for all tested configurations. This confirms that the observed magnitude scaling and tectonic offsets are not artifacts of a particular spatiotemporal window choice, but reflect robust, first-order properties of global aftershock productivity.

Mainshocks occurring deeper than 100 km were retained but explicitly tracked for depth-dependent analyses. Aftershocks were not declustered, as the objective of this study is to characterize the full cascading productivity of each large earthquake. In this study, the term aftershock productivity is used in an operational and observational sense, defined as the number of cataloged earthquakes exceeding a fixed magnitude threshold within a prescribed space–time window following each mainshock. This definition differs from the formal ETAS productivity parameter, which represents the expected number of directly triggered offspring events in an idealized branching process and depends explicitly on magnitude-dependent spatial and temporal kernels. However, because some $Mw \geq 7.0$ earthquakes may themselves occur within the aftershock sequence of an earlier, larger event, treating all $Mw \geq 7.0$ earthquakes as independent mainshocks may introduce statistical dependence and double counting of triggered events. To ensure statistical independence of the analyzed mainshocks, we explicitly distinguish between descriptive and inferential uses of the $Mw \geq 7.0$ catalog. All $Mw \geq 7.0$ earthquakes are retained when illustrating spatial distributions and global seismotectonic patterns. However, for all analyses that assume independent triggering—including magnitude–productivity regressions, correlation analyses, and hypothesis testing—we restrict the dataset to a subset of independent mainshocks. To explicitly address this issue, we identify and flag all $Mw \geq 7.0$ events that occur within the spatiotemporal aftershock window ($r \leq 200$ km, $t \leq 30$ days) of a preceding larger mainshock. These events are retained in the catalogue for descriptive analyses, but are excluded from all regression, correlation, and hypothesis-testing procedures that assume statistical independence of mainshocks. This filtering prevents double counting of triggered seismicity and

https://doi.org/10.5194/egusphere-2026-877
Preprint. Discussion started: 22 June 2026

ensures that each aftershock sequence is uniquely associated with a single causative mainshock in all statistical analyses. All statistical results reported in following Sections are therefore based exclusively on a filtered set of independent mainshocks. This filtering step also reduces the artificial inflation of productivity estimates that would otherwise arise from overlapping aftershock sequences of temporally clustered large earthquakes.

For each mainshock, aftershock productivity N was defined as the total number of earthquakes satisfying:

- Mw_after ≥ 4.5
- $0 \leq \Delta t \leq 30$ days
- hypocentral distance ≤ 200 km

To regularize the distribution and avoid zero-count issues, we analyzed productivity in log-space using:

$$\log_{10}(N + 1) \quad (1)$$

The use of the log10(N+1) transformation follows common practice in aftershock and triggering studies, where productivity distributions are strongly right-skewed and may include zero-count cases. Excluding mainshocks with no detected aftershocks would introduce a systematic bias toward more productive events and artificially inflate productivity estimates, particularly for intraplate earthquakes. The log(N+1) formulation allows all mainshocks to be retained while preserving relative scaling relationships. Because any truncation effects associated with the fixed window scale monotonically with mainshock magnitude, they primarily affect the intercept of the productivity relation rather than its slope, and therefore do not invalidate comparative analyses of scaling behavior across tectonic classes.

This transformation preserves relative scaling while stabilizing variance and enabling the use of standard linear regression and parametric statistical tests.

https://doi.org/10.5194/egusphere-2026-877
Preprint. Discussion started: 22 June 2026

To classify each mainshock into tectonic domains, we used the PB2002 global plate-boundary model (Bird, 2003), including subduction interfaces, transform boundaries, and divergent boundaries. The PB2002 dataset was projected into a metric coordinate system (EPSG:3857) to compute distances in meters along the Earth's surface.

For each event we calculated the minimum distance to the nearest plate boundary:

$$d_{\mathrm{PB}} = \min_i \left[\mathrm{dist}(\mathrm{mainshock}, \mathrm{PB}_i)\right] \quad (2)$$

Tectonic classes were defined as:

- Subduction – events located ≤ 200 km from a PB2002 subduction interface,
- Other plate boundary – events located ≤ 200 km from any non-subduction plate boundary,
- Intraplate/Crustal – events located > 200 km from any PB2002 boundary.

This three-class scheme is consistent with global seismotectonic frameworks and allows tectonic setting to be treated as a categorical variable in subsequent analyses.

To quantify the dependence of aftershock productivity on mainshock magnitude, we performed ordinary least squares (OLS) regressions of the form

$$\log_{10}(N+1) = a + b\,Mw \quad (3)$$

computed independently for each tectonic class and for the full global sample. For each regression we estimated:

- slope b,
- intercept a,
- standard errors and p-values,
- coefficient of determination R^2.

https://doi.org/10.5194/egusphere-2026-877
Preprint. Discussion started: 22 June 2026

These regressions provide both a global magnitude–productivity scaling and class-specific offsets. To further verify temporal robustness, we repeated the magnitude–productivity analysis for different sub-periods of the catalog and found consistent slopes and intercept ordering among tectonic classes. This confirms that the observed relationships are stable through time and not driven by temporal changes in catalog quality. In this sense, our results provide global empirical constraints on the magnitude scaling and tectonic modulation of aftershock productivity that can inform, but do not replace, the parameterization of physics-based or ETAS-type seismicity models. The regression residuals,

$$\varepsilon = \log_{10}(N+1) - (a + b\,Mw) \quad (4)$$

were then used to examine secondary controls from depth and distance to plate boundaries after removing the primary Mw dependence.

To formally test whether aftershock productivity differs among tectonic domains, we applied both parametric and non-parametric statistics:

1. One-way ANOVA on $\log_{10}(N+1)$ across the three tectonic classes;
2. Kruskal–Wallis tests as a distribution-free counterpart.

These statistical tests are used here as complementary diagnostics to support patterns already evident in the regression analyses and distributional comparisons. Given the limited sample size and the intrinsic variability of aftershock sequences, p-values are interpreted cautiously and in conjunction with effect sizes, confidence intervals, and physical consistency across multiple independent analyses. Where global tests indicated significant differences, we performed post-hoc pairwise comparisons:

- Tukey's honestly significant difference (HSD) test following ANOVA,
- Dunn's test with Holm correction following Kruskal–Wallis.

https://doi.org/10.5194/egusphere-2026-877
Preprint. Discussion started: 22 June 2026

We applied the same framework both to $\log_{10}(N+1)$and to regression residuals, to distinguish between differences driven directly by magnitude scaling and those related to additional source- or environment-dependent effects.

To assess how depth and plate-boundary proximity modulate aftershock productivity beyond magnitude and tectonic class, we examined relationships between productivity (and residuals) and:

- mainshock depth,
- distance to the nearest plate boundary d_{PB}.

We computed:

- scatter plots of $\log_{10}(N+1)$and residuals versus depth and d_{PB},
- locally weighted regression (LOWESS) curves to highlight non-linear trends,
- binned statistics in distance classes (e.g., 0–50 km, 50–150 km, >150 km),
- distributional summaries (violin, box, and swarm plots) of d_{PB}, N, $\log_{10}(N+1)$, e residuals for each tectonic class.

These analyses allow us to quantify whether depth and plate-boundary distance introduce systematic, magnitude-normalized trends in aftershock productivity.

To explore how magnitude, depth, plate-boundary distance, productivity, and residuals co-vary in a multivariate sense, we computed:

- Pearson correlation matrices among all key variables,
- pairwise joint distributions (pairplots) with kernel density estimates,
- two-dimensional Mw–depth productivity maps, where median $\log_{10}(N+1)$was evaluated in Mw–depth bins.

These multivariate diagnostics complement the regression-based analysis and help identify whether any additional structure remains unexplained by magnitude and tectonic setting alone.

https://doi.org/10.5194/egusphere-2026-877
Preprint. Discussion started: 22 June 2026

3. Results

The global catalogue of 561 Mw ≥ 7 earthquakes displays a clear spatial clustering along major plate boundaries, with subduction megathrusts dominating the western Pacific, South America, and Indonesia, while intraplate and crustal events are comparatively sparse and regionally localized (Figure 1). The three tectonic classes—subduction, other plate-boundary, and intraplate/crustal—show distinct geographical patterns consistent with global plate kinematics (Bird, 2003; Kagan & Jackson, 2014).

Across all tectonic settings, aftershock productivity increases systematically with mainshock magnitude. Scatterplots with OLS regressions (Figure 2) show robust positive slopes in each tectonic class, with limited scatter at the highest magnitudes (Mw ≥ 8.5). A direct comparison of the three regression lines (Figure 3) demonstrates broadly similar slopes ($b \approx 0.76–0.81$), while intercepts differ, indicating higher aftershock productivity in subduction zones for a given Mw. Table 1 reports regression coefficients and R^2 values.

These results confirm a universal magnitude scaling, consistent with prior global studies (Utsu, 1970; Helmstetter, 2003; Shearer, 2012; van der Elst & Shaw, 2015), but highlight systematic offsets controlled by tectonic setting.

Figure 4 shows aftershock productivity as a function of mainshock depth. Subduction and boundary events exhibit mild decreases at depths >50–60 km, while intraplate events display more gradual, heterogeneous trends. Depth explains only modest variance in productivity relative to magnitude.

Figure 5 examines the distance to the nearest PB2002 plate boundary. Subduction and other boundary events cluster tightly within <150 km of a plate boundary, reflecting their tectonic context, while intraplate events span distances >1,000 km. Only the intraplate class shows a weak but systematic decrease in productivity at intermediate distances (200–1,200 km), though scatter remains high. This suggests that continental intraplate stress regimes may influence rupture fragmentation and secondary triggering (Scholz, 2019; Craig et al., 2016).

https://doi.org/10.5194/egusphere-2026-877
Preprint. Discussion started: 22 June 2026

To isolate the effects of depth and tectonic setting from the dominant Mw scaling, we analyze residuals from class-specific regressions (Table 1). Residuals vs depth (Figure 6) show small, non-monotonic trends with amplitudes <0.2 log units, indicating only weak depth dependence after magnitude normalization.

Residuals vs distance to plate boundaries (Figure 7) again show negligible systematic variations for subduction and other boundary events, whereas intraplate events exhibit a shallow minimum at ~200–300 km. Overall, residual amplitudes remain within ±0.5 log units, confirming that Mw and tectonic setting dominate productivity patterns.

Statistical tests provide independent confirmation of patterns identified through regression and distributional analyses, rather than serving as the primary basis for interpretation. ANOVA and Kruskal–Wallis tests (Table 2) indicate significant differences among classes for $\log_{10}(N+1)$ but not for residuals. Tukey and Dunn post-hoc tests (Table 3) show that subduction differs significantly from both other classes, while boundary vs intraplate differences are not significant—again consistent with Figure 3.

Violin plots of distance to PB2002 boundaries (Figure 8) illustrate the expected separation among tectonic classes: subduction events occur closest to boundaries, boundary-other events at intermediate distances, and intraplate events farthest away (often >1,000 km).

Raw aftershock counts (Figure 9) differ substantially across classes, with subduction zones hosting the highest absolute numbers and intraplate earthquakes showing both lower medians and greater variability. However, when transformed to $\log_{10}(N+1)$ (Figure 10), the distributions become more comparable, emphasizing the multiplicative nature of aftershock productivity and its dependence on Mw.

Residual distributions (Figure 11) demonstrate that, once normalized for Mw, differences among tectonic classes are strongly reduced, consistent with statistical tests (Tables 2–3).

The Pearson correlation matrix (Figure 12) shows that Mw is the dominant predictor of aftershock productivity ($r \approx 0.48$ with $\log_{10}(N+1)$); depth and distance to boundaries display weak correlations

https://doi.org/10.5194/egusphere-2026-877
Preprint. Discussion started: 22 June 2026

($|r| < 0.13$). Residuals remain strongly correlated with $\log_{10}(N+1)$ due to shared variance from Mw-regression uncertainty.

The multidimensional pairplot (Figure 13) highlights the strong clustering by tectonic class and confirms that depth and distance partly separate the three groups. Nonetheless, their impact on aftershock productivity is secondary to magnitude and tectonic class.

The Mw–depth heatmap (Figure 14) synthesizes the two-dimensional structure of aftershock productivity. Median $\log_{10}(N+1)$ increases sharply with magnitude across all depths. Depth variations appear only at second order: shallow events (0–40 km) are slightly more productive, whereas deep events (>60 km) produce fewer aftershocks for the same Mw. These patterns reinforce the conclusion that Mw and tectonic setting are the primary first-order controls on global aftershock productivity. Accordingly, the robustness of the results is established through the convergence of multiple lines of evidence—regression scaling, residual behavior, distributional consistency, and multivariate structure—rather than reliance on any single statistical test.

Across all analyses, three robust conclusions emerge:

1. Magnitude is the dominant global control, governing the first-order scaling of aftershock productivity and explaining most of the variance in $\log_{10}(N+1)$. The near-linear Mw–productivity relationship (Figures 2–3; Table 1) is globally consistent across tectonic environments.
2. Tectonic setting exerts a strong secondary influence, primarily manifested as systematic differences in intercept (baseline productivity). At the same magnitude, subduction megathrust earthquakes produce substantially more aftershocks than other plate-boundary events, which in turn exceed intraplate/crustal earthquakes (Figures 2–4; Table 2).
3. Depth and distance exert weaker, context-dependent influences, becoming significant mainly for deeper (≥40–60 km) or intraplate events. Productivity and regression residuals decrease systematically with depth (Figures 4 & 6), while distance to the nearest plate boundary modulates scatter primarily for intraplate earthquakes (Figures 5 & 7). Correlation matrices

https://doi.org/10.5194/egusphere-2026-877
Preprint. Discussion started: 22 June 2026

and multivariate distributions (Figures 12–13) confirm that these parameters contribute only modestly to global variance relative to Mw and tectonic setting.

4. Discussion

Our global analysis reveals a remarkably consistent scaling of aftershock productivity with mainshock magnitude, alongside systematic differences associated with tectonic environment. Together, these findings clarify long-standing ambiguities in the interpretation of global aftershock statistics and provide a unified physical framework for understanding why earthquakes of similar magnitude may produce vastly different aftershock sequences.

The near-linear Mw–productivity scaling identified in Figures 2–3 confirms that magnitude is the dominant global predictor of aftershock productivity. The slope values ($b \approx 0.76–0.81$) fall within the range predicted by rate-and-state models and observed in regional studies (e.g., Helmstetter 2003; Nandan et al., 2017; Page et al., 2016), supporting the interpretation that the number of triggered events is fundamentally governed by the size of the stress perturbation and the effective size of the failure zone.

The fact that the slope is essentially invariant across tectonic settings reinforces the idea that the magnitude scaling reflects a universal triggering mechanism, likely controlled by rupture geometry, stress drop, and fault-zone rheology (Kanamori & Anderson, 1975; Scholz, 2019). This invariance also explains why ETAS productivity parameters tend to cluster globally, despite strong regional differences in background seismicity and faulting style.

Although magnitude determines the first-order scaling, Figures 2–4 and Tables 1–2 show that tectonic setting produces clear, reproducible offsets in baseline productivity. For a given Mw:

- Subduction earthquakes are the most productive;
- Other plate-boundary earthquakes show intermediate productivity;
- Intraplate/crustal earthquakes systematically produce fewer aftershocks.

https://doi.org/10.5194/egusphere-2026-877
Preprint. Discussion started: 22 June 2026

These distinctions likely arise from persistent physical differences among tectonic domains. Subduction megathrusts are characterized by high degrees of structural heterogeneity, large fault-zone widths, elevated pore-fluid pressures, and high thermal gradients—conditions favorable to sustained triggering and efficient stress transfer (Lay & Kanamori, 1981; Hayes et al., 2012). In contrast, intraplate faults tend to be more isolated, colder, and less fractured, reducing the density of failure-ready asperities.

The fact that tectonic setting expresses itself primarily through intercept shifts rather than slope changes suggests that the physical mechanisms controlling the absolute number of aftershocks differ among tectonic domains, but the magnitude dependence remains universal. This reconciles contrasting findings in earlier studies, which variously emphasized tectonic differences (e.g., Das & Henry 2003; Scholz 2019) or magnitude-controlled universality (e.g., Felzer et al., 2004).

Figures 4–5 show that depth and distance to the nearest plate boundary have much weaker effects, but they are not negligible. Depth-dependent productivity decay—most evident below 40–60 km—corroborates earlier findings linking aftershock rates to lithospheric temperature, confining pressure, and frictional stability (Sibson, 1982; Houston, 2015). The systematic decay of residuals with depth (Figure 6) indicates that deeper ruptures increasingly occur in conditions that inhibit secondary failure, such as higher normal stresses and more ductile rheology.

Distance to plate boundaries primarily affects intraplate events (Figures 7–8), likely reflecting the decreasing availability of optimally oriented faults and the relative mechanical isolation of continental interiors. Yet correlations remain weak (Figure 12), confirming that distance-based effects are secondary compared to consistently strong controls from Mw and tectonic setting.

These results have direct implications for global hazard modeling, operational aftershock forecasting, and ETAS parameterization.

1. Magnitude-dependent triggering can be modeled globally with a single slope, reducing epistemic uncertainty and simplifying global forecasting frameworks.

https://doi.org/10.5194/egusphere-2026-877
Preprint. Discussion started: 22 June 2026

2. Tectonic-class-specific intercepts provide a natural way to introduce physically grounded regionalization without overfitting.
3. Depth-dependent corrections may be necessary for intermediate- and deep-focus earthquakes, which are systematically underproductive relative to crustal ruptures.
4. The weak influence of distance to plate boundaries confirms that intraplate sequence productivity is inherently low, not simply the result of catalog bias.

Overall, our results bridge the gap between global-scale empirical patterns and the physical processes that govern earthquake triggering across tectonic environments.

5. Conclusions

This study presents a global-scale, data-driven quantification of aftershock productivity that jointly evaluates the roles of magnitude, tectonic setting, depth, and distance to plate boundaries using a uniformly processed catalog of Mw ≥ 7 earthquakes (1976–2024). Several robust conclusions emerge:

1. Magnitude is the primary global control on aftershock productivity. The Mw–$\log_{10}(N+1)$ relation exhibits a consistent slope across tectonic settings, demonstrating universal scaling.
2. Tectonic setting exerts a strong secondary influence, expressed as systematic offsets among subduction, other plate-boundary, and intraplate events. These offsets reflect persistent physical differences in fault-zone properties and seismogenic conditions.
3. Depth and distance provide weaker, context-dependent modulation, with productivity decreasing at depths >40–60 km and for intraplate events far from plate boundaries.
4. Residual analysis and multivariate correlations confirm that Mw and tectonic domain explain the vast majority of global variance, whereas depth and distance contribute only modestly.
5. These findings establish a coherent, physically interpretable global framework for aftershock productivity. They also provide practical guidance for improving global ETAS

https://doi.org/10.5194/egusphere-2026-877
Preprint. Discussion started: 22 June 2026

parameterization, seismic hazard assessments, and rapid aftershock forecasts in future large earthquakes.

The global separation of magnitude-driven scaling and tectonic-domain intercepts offers a promising path toward hybrid physical–statistical models capable of capturing both universal and environment-specific aspects of earthquake triggering.

Data statement

Earthquake origin times, locations, depths, and magnitudes were obtained from the U.S. Geological Survey (USGS) ComCat earthquake catalog, accessed via the ComCat API (https://earthquake.usgs.gov/fdsnws/event/1/; last accessed in 2025). The catalog was queried for global earthquakes with Mw ≥ 7.0 occurring between 1976 and 2024.

Plate boundary geometries used to classify earthquakes into tectonic settings were taken from the PB2002 global plate boundary model (Bird, 2003), available at https://peterbird.name/oldFTP/PB2002/ (last accessed in 2025).

All data processing, statistical analyses, and figure generation were performed using custom Python scripts developed by the authors. Calculations relied on open-source Python libraries including NumPy, Pandas, SciPy, Statsmodels, GeoPandas, Matplotlib, and Seaborn. No proprietary software or restricted-access datasets were used in this study.

Declaration of Competing Interests

The authors declare no competing interests.

Acknowledgments

We acknowledge the agencies and institutions that maintain the global seismic catalogs and plate-boundary datasets used in this study, whose sustained efforts make large-scale, reproducible

https://doi.org/10.5194/egusphere-2026-877
Preprint. Discussion started: 22 June 2026

seismological research possible. We thank the developers and maintainers of open-source scientific software used for data processing, analysis, and visualization. This research received no specific grant from any funding agency in the public, commercial, or not-for-profit sectors.

6. References

Bird, P., 2003. An updated digital model of plate boundaries. Geochemistry, Geophysics, Geosystems 4, 1027. https://doi.org/10.1029/2001GC000252

Craig, T.J., Copley, A.C., Middleton, T., 2017. Constraining fault friction in intraplate earthquakes. Geophysical Journal International 208, 1642–1664.

Das, S., Scholz, C.H., 1981. Theory of large intraplate earthquakes. Science 213, 1153–1160.

Ekström, G., Nettles, M., Dziewoński, A.M., 2012. The global CMT project 2004–2010: Centroid-moment tensors for 13,017 earthquakes. Phys. Earth Planet. Inter. 200–201.

Felzer, K.R., Becker, T.W., Abercrombie, R.E., 2002. Correlation between aftershock productivity and earthquake stress drops. Geophysical Research Letters 29, 2286.

Hainzl, S., 2016. Rate-dependent incompleteness of earthquake catalogs. Seismological Research Letters 87, 337–344.

Hainzl, S., Moradpour, J., Davidsen, J., 2016. Aftershock generation as dependent on mainshock rupture properties. Journal of Geophysical Research 121, 2575–2590.

https://doi.org/10.5194/egusphere-2026-877
Preprint. Discussion started: 22 June 2026

Hayes, G.P., Wald, D.J., Johnson, R.L., 2012. Slab1.0: Global 3-D subduction geometry. Journal of Geophysical Research 117, B01302.

Hayes, G.P., Moore, G.L., Portner, D.E., et al., 2018. Slab2: A comprehensive subduction zone geometry model. Geochemistry, Geophysics, Geosystems 19, 4469–4503.

Hayes, G.P., et al., 2020. The global development of NEIC moment tensor solutions. Seismological Research Letters 91, 2230–2243.

Helmstetter, A., 2003. Is earthquake triggering driven by small earthquakes? Physical Review Letters 91, 058501.

Helmstetter, A., Sornette, D., 2003. Predictability in the ETAS model. Journal of Geophysical Research 108, 2482.

Kanamori, H., Brodsky, E.E., 2004. The physics of earthquakes. Reports on Progress in Physics 67, 1429–1496.

Lay, T., Kanamori, H., 2011. Insights from the great 2011 Japan earthquake. Physics Today 64, 33–39.

Lay, T., Ammon, C.J., Kanamori, H., et al., 2005. Rupture characteristics of megathrust earthquakes. Science 308, 1127–1134.

Lima, R.G., Courboulex, F., Cotton, F., 2021. Aftershock productivity across global regions. Bulletin of the Seismological Society of America 111, 1531–1547.

https://doi.org/10.5194/egusphere-2026-877
Preprint. Discussion started: 22 June 2026

Marzocchi, W., Lombardi, A.M., 2009. Real-time aftershock forecasting using ETAS. Bulletin of the Seismological Society of America 99, 172–189.

Marsan, D., Lengliné, O., 2008. Extending aftershock triggering models with near-field interactions. Journal of Geophysical Research 113, B09304.

Nishimura, T., Uchide, T., Sekiguchi, H., 2020. Rupture complexity and aftershock productivity in Japan. Earth, Planets and Space 72, 1–15.

Ogata, Y., 1998. Space-time point-process models for earthquake clustering. Annals of the Institute of Statistical Mathematics 50, 379–402.

Omi, T., Ogata, Y., Hirata, Y., Aihara, K., 2013. Forecasting large aftershocks with ETAS models. Journal of Geophysical Research 118, 3642–3653.

Omori, F., 1894. On the aftershocks of earthquakes. Journal of the College of Science, Imperial University of Tokyo 7, 111–200.

Page, M.T., van der Elst, N.J., Hardebeck, J.L., Felzer, K.R., 2016. Optimal forecasting of aftershock activity. Journal of Geophysical Research 121, 5088–5108.

Parsons, T., 2002. Global Omori law decay of triggered earthquakes. Journal of Geophysical Research 107, 2199.

https://doi.org/10.5194/egusphere-2026-877
Preprint. Discussion started: 22 June 2026

Reasenberg, P.A., Jones, L.M., 1994. Earthquake aftershock occurrence: Relations to mainshock magnitude. Journal of Geophysical Research 99, 6527–6540.

Scholz, C.H., 2002. The Mechanics of Earthquakes and Faulting. Cambridge University Press.

Scholz, C.H., 2019. Mechanisms of intraplate earthquakes. Nature Communications 10, 1–10.

Shcherbakov, R., Turcotte, D.L., Rundle, J.B., 2004. A generalized Omori law. Physical Review Letters 93, 178501.

Stein, S., Okal, E.A., 2007. Ultralong aftershock sequences of great earthquakes. Science 316, 1737.

Uchide, T., Imanishi, K., Nakai, M., et al., 2013. Aftershock productivity and mainshock complexity in Japan. Earth, Planets and Space 65, 1607–1612.

Utsu, T., 1961. A statistical study on the occurrence of aftershocks. Geophys. Mag. 30, 521–605.

Utsu, T., Ogata, Y., Matsu'ura, R.S., 1995. The centenary of the Omori formula. Journal of Physics of the Earth 43, 1–33.

van der Elst, N.J., 2021. Aftershock productivity linked to stress drop variability. Journal of Geophysical Research 126, e2020JB021145.

van der Elst, N.J., Page, M.T., 2014. Aftershock productivity and background seismicity rate. Geophysical Research Letters 41, 8460–8467.

https://doi.org/10.5194/egusphere-2026-877
Preprint. Discussion started: 22 June 2026

587 Wells, D.L., Coppersmith, K.J., 1994. New empirical relationships among magnitude, rupture length,
588 rupture width. Bull. Seismol. Soc. Am. 84, 974–1002.
589
590 Wilcock, W.S.D., Tolstoy, M., Waldhauser, F., et al., 2009. Seismicity of mid-ocean ridges. Nature
591 Geoscience 2, 646–652.
592
593 Zhuang, J., Ogata, Y., Vere-Jones, D., 2004. Analyzing earthquake clustering with ETAS. Journal of
594 Geophysical Research 109, B05301.

https://doi.org/10.5194/egusphere-2026-877
Preprint. Discussion started: 22 June 2026

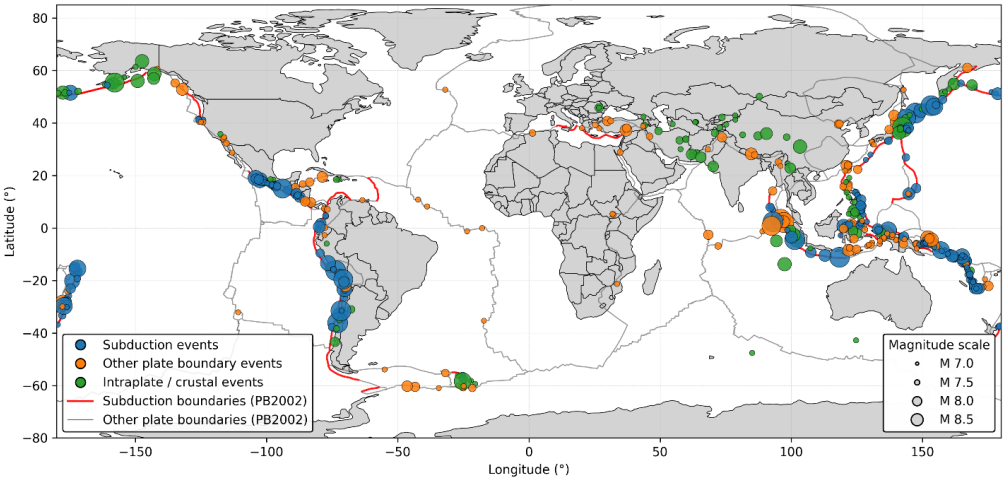

Figure 1. *Global distribution of Mw ≥ 7 mainshocks considered in this study (1976–2024). Colors indicate tectonic setting—subduction megathrusts (blue), other plate-boundary events (orange), and intraplate/crustal earthquakes (green)—with symbol size proportional to mainshock magnitude. Plate boundaries from PB2002 (red = subduction, grey = other boundary types) are shown for reference.*

https://doi.org/10.5194/egusphere-2026-877
Preprint. Discussion started: 22 June 2026

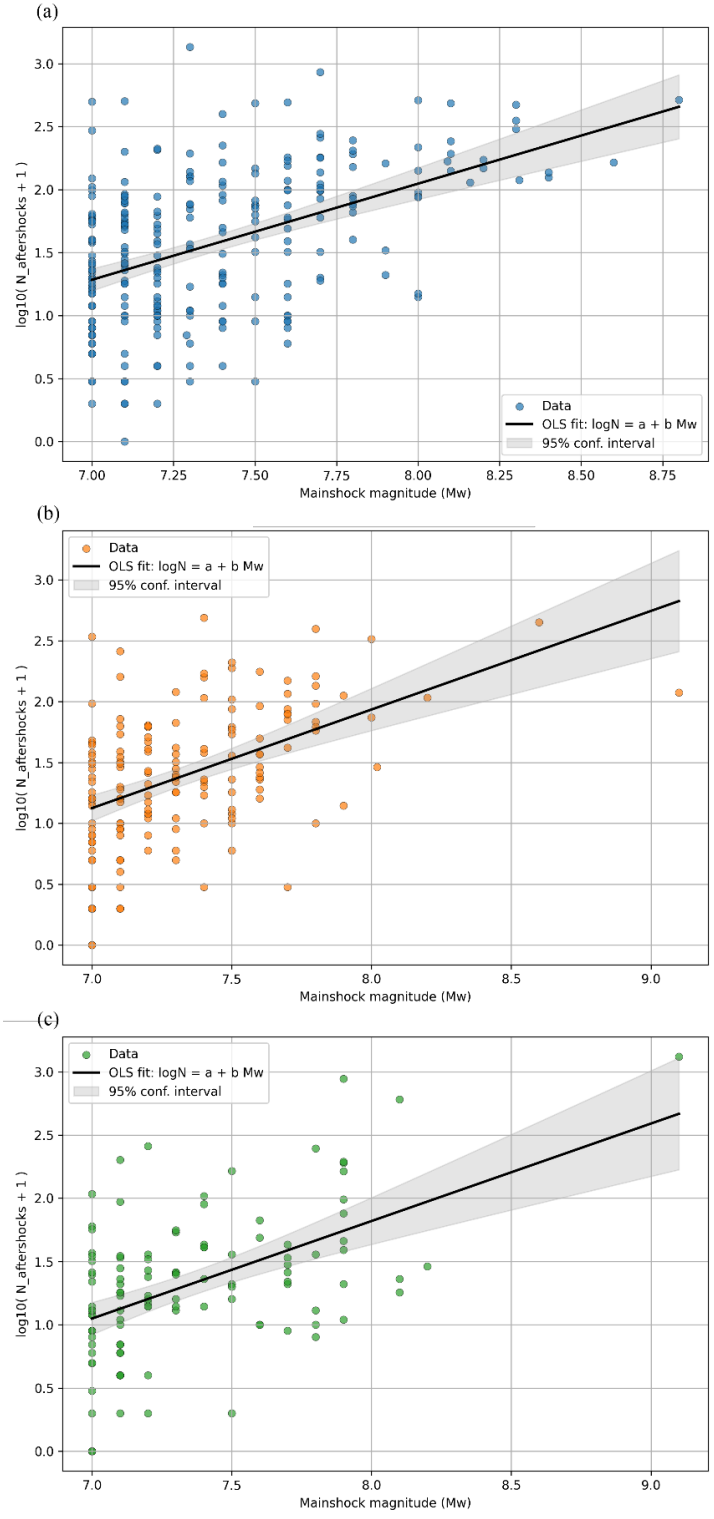

https://doi.org/10.5194/egusphere-2026-877
Preprint. Discussion started: 22 June 2026

Figure 2. *Aftershock productivity as a function of mainshock moment magnitude for the three tectonic settings. Panels show $\log_{10}$(N aftershocks + 1) versus Mw for: (a) subduction, (b) other plate-boundary, and (c) intraplate/crustal earthquakes. Each panel includes an ordinary-least-squares (OLS) regression $\log_{10}(N + 1) = a + bMw$ (black line) with 95% confidence interval (grey shading). Systematic differences in intercept and slope highlight distinct productivity behaviors across tectonic environments.*

https://doi.org/10.5194/egusphere-2026-877
Preprint. Discussion started: 22 June 2026

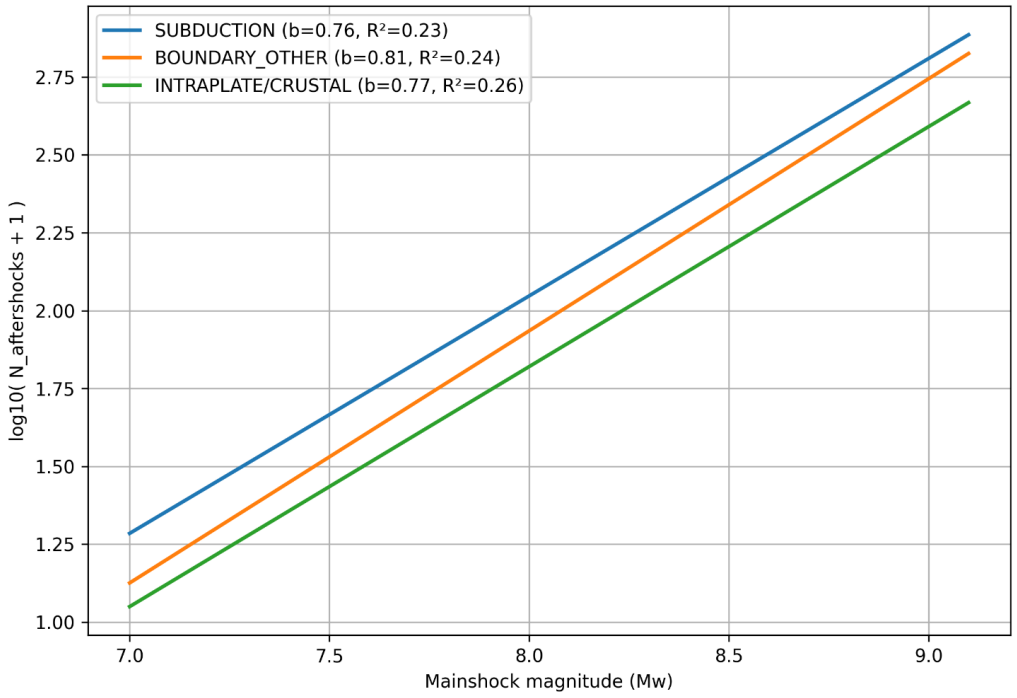

Figure 3. *Comparison of OLS regression lines for aftershock productivity across the three tectonic settings. Regression curves (with slope b and R² reported in the legend) summarize the scaling* $\log_{10}(N + 1) = a + bMw$ *for subduction, other plate-boundary, and intraplate/crustal earthquakes. Subduction events exhibit the highest baseline productivity (largest intercept), whereas intraplate events show the lowest.*

https://doi.org/10.5194/egusphere-2026-877
Preprint. Discussion started: 22 June 2026

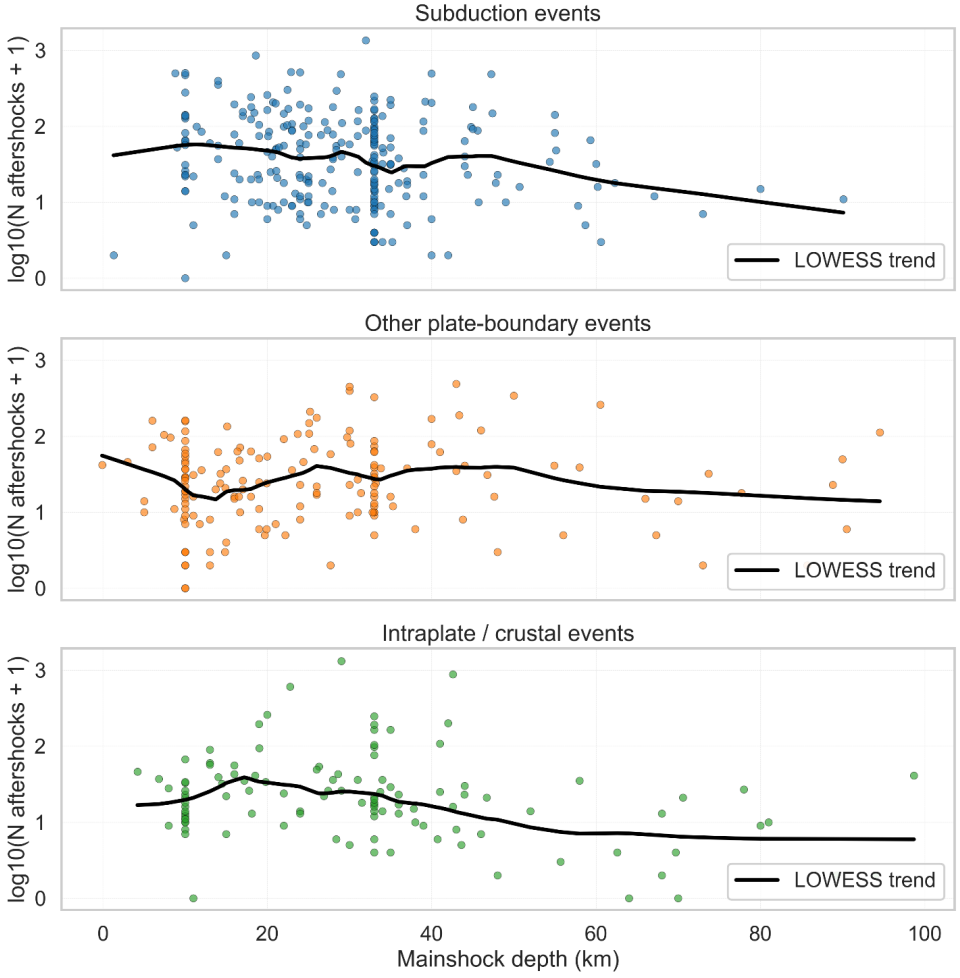

Figure 4. *Aftershock productivity versus mainshock focal depth for the three tectonic settings. Scatter points show $\log_{10}(N + 1)$ as a function of depth, with a LOWESS trend (black line) illustrating non-parametric variations. All classes display weak depth dependence, with a slight decrease in productivity for deeper events, especially >60 km.*

https://doi.org/10.5194/egusphere-2026-877
Preprint. Discussion started: 22 June 2026

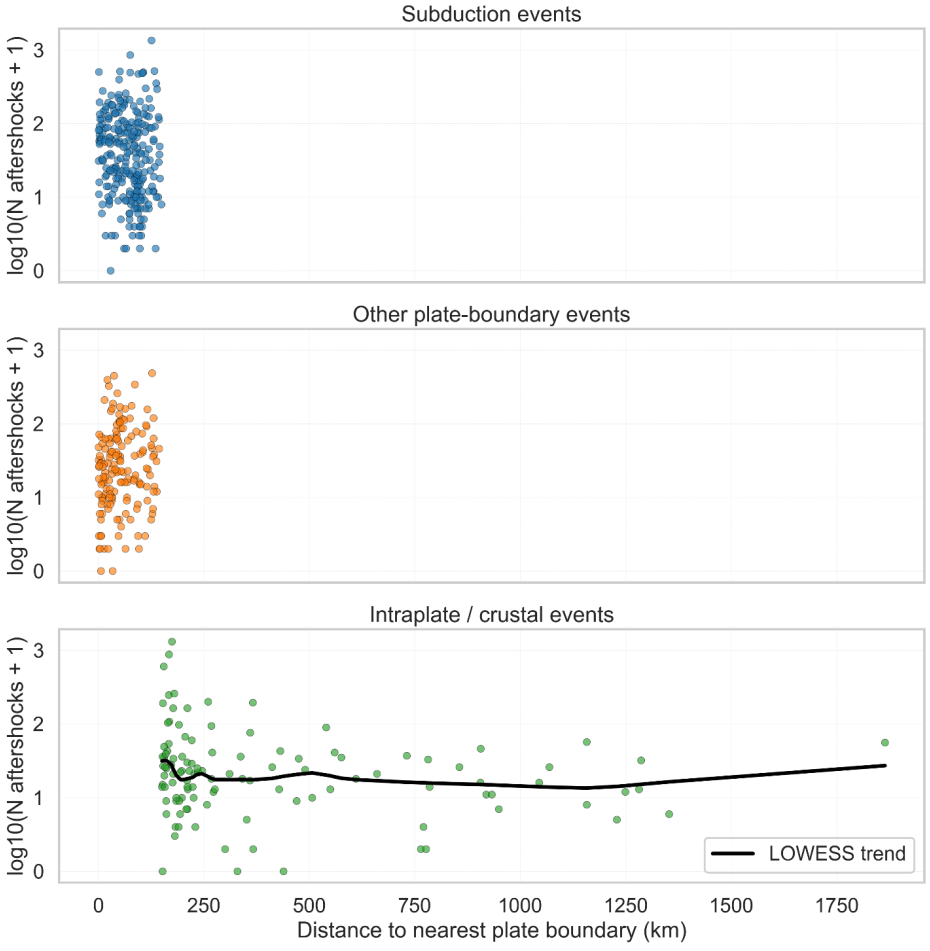

Figure 5. *Aftershock productivity versus distance from the nearest PB2002 plate boundary. Panels show $\log_{10}(N + 1)$ for the three tectonic environments. Subduction and other plate-boundary events cluster within small distances (0–100 km), whereas intraplate events span >1500 km. A LOWESS trend is shown only where data coverage permits (intraplate). Productivity decreases moderately with increasing distance from plate boundaries for intraplate earthquakes.*

https://doi.org/10.5194/egusphere-2026-877
Preprint. Discussion started: 22 June 2026

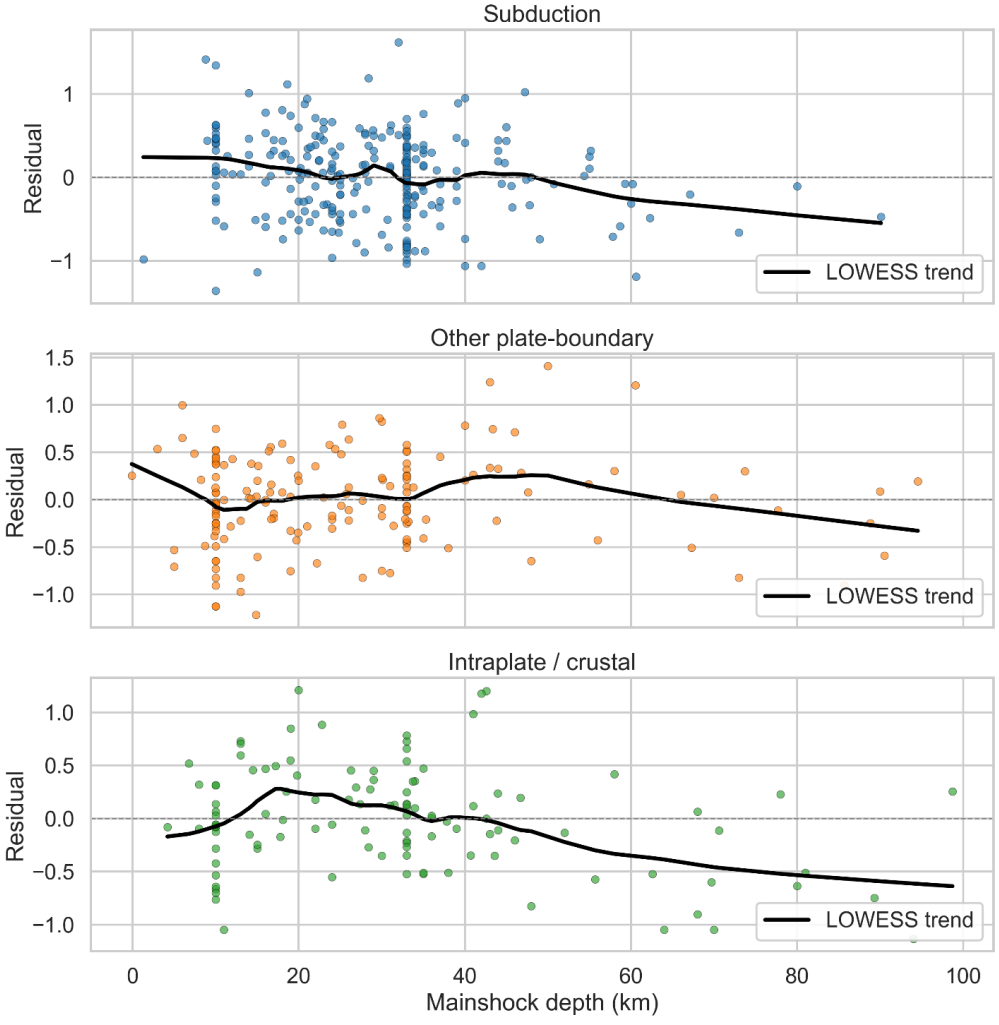

Figure 6. *Regression residuals (observed – predicted $\log_{10}(N + 1)$) versus mainshock focal depth. LOWESS curves highlight depth-dependent deviations from the magnitude–productivity scaling. Residuals tend to be slightly positive at shallow depths in subduction and intraplate settings, and decrease systematically at depths >60 km.*

https://doi.org/10.5194/egusphere-2026-877
Preprint. Discussion started: 22 June 2026

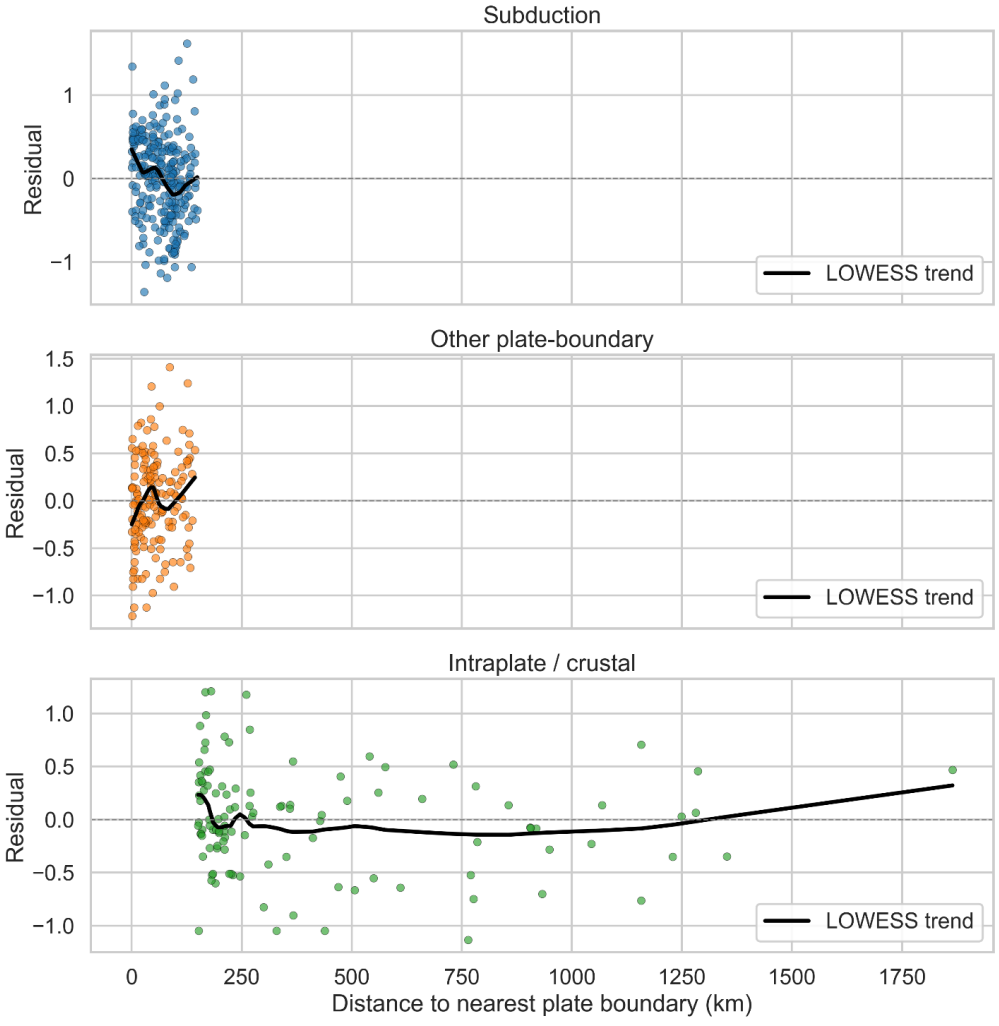

Figure 7. *Regression residuals versus distance to the nearest PB2002 plate boundary. Panels illustrate deviations from the Mw-based scaling across tectonic settings. A mild decrease in residuals with increasing distance is visible in the intraplate class, whereas boundary and subduction events show limited variability because their distances cluster near zero.*

https://doi.org/10.5194/egusphere-2026-877
Preprint. Discussion started: 22 June 2026

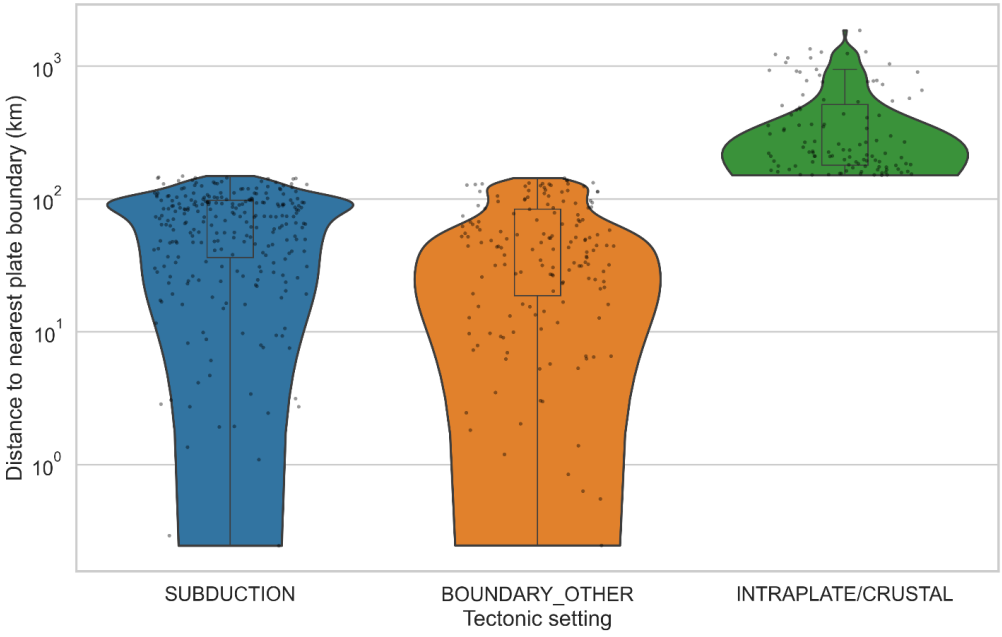

Figure 8. *Distribution of mainshock distances to plate boundaries for the three tectonic classes. Violin plots display the full distribution with embedded boxplots. Subduction and other boundary events occur predominantly within 100 km of plate boundaries, whereas intraplate earthquakes show a broad distribution extending beyond 1500 km.*

https://doi.org/10.5194/egusphere-2026-877
Preprint. Discussion started: 22 June 2026

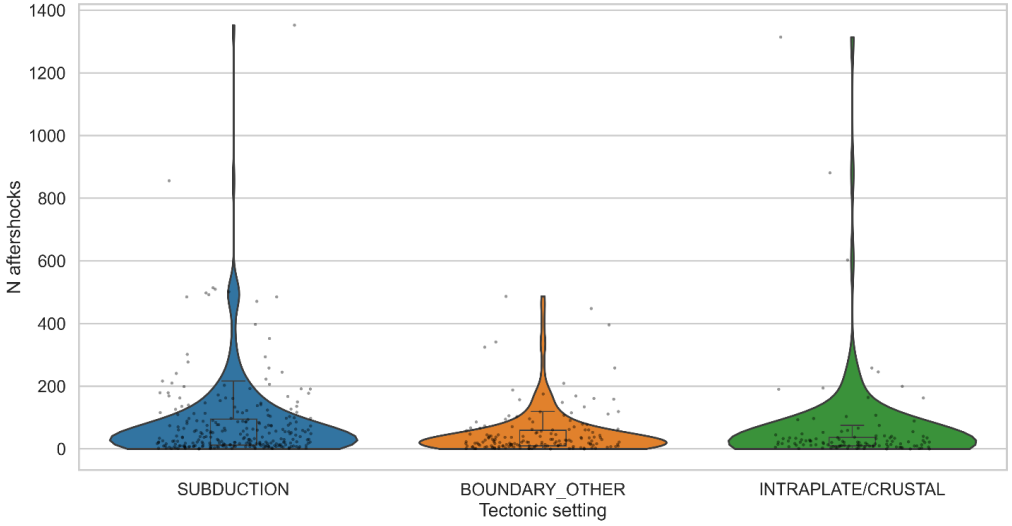

Figure 9. *Distribution of raw aftershock counts N for the three tectonic settings. Violin plots show that subduction earthquakes produce the largest number of aftershocks, followed by intraplate and other plate-boundary events. Long-tailed distributions reflect occasional highly productive sequences.*

https://doi.org/10.5194/egusphere-2026-877
Preprint. Discussion started: 22 June 2026

646

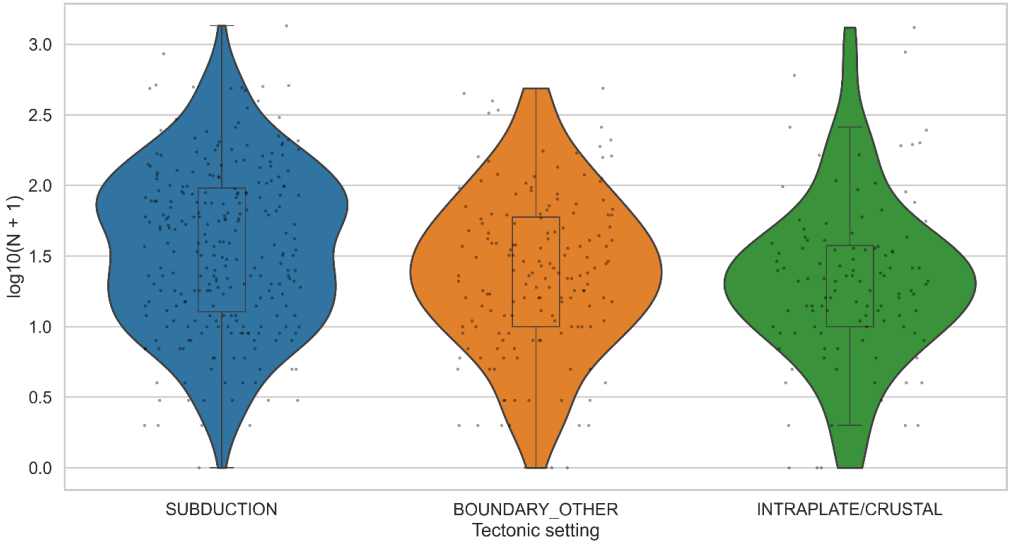

647

648 **Figure 10.** *Distribution of $\log_{10}(N + 1)$ aftershock productivity across tectonic settings. Log-*
649 *transformed counts emphasize systematic differences in baseline productivity: subduction events*
650 *exhibit the highest median values, intraplate intermediate, and other plate-boundary the lowest.*

https://doi.org/10.5194/egusphere-2026-877
Preprint. Discussion started: 22 June 2026

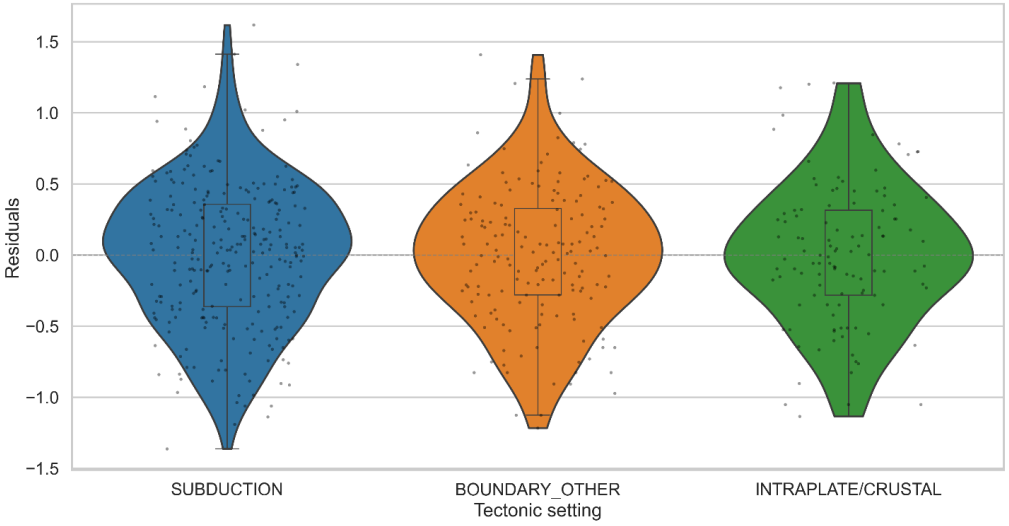

Figure 11. *Distribution of regression residuals across the three tectonic settings. Violin plots show that subduction earthquakes have slightly positive median residuals, consistent with higher-than-predicted productivity. Boundary events cluster near zero, whereas intraplate events show a broader spread with slightly negative tails.*

https://doi.org/10.5194/egusphere-2026-877
Preprint. Discussion started: 22 June 2026

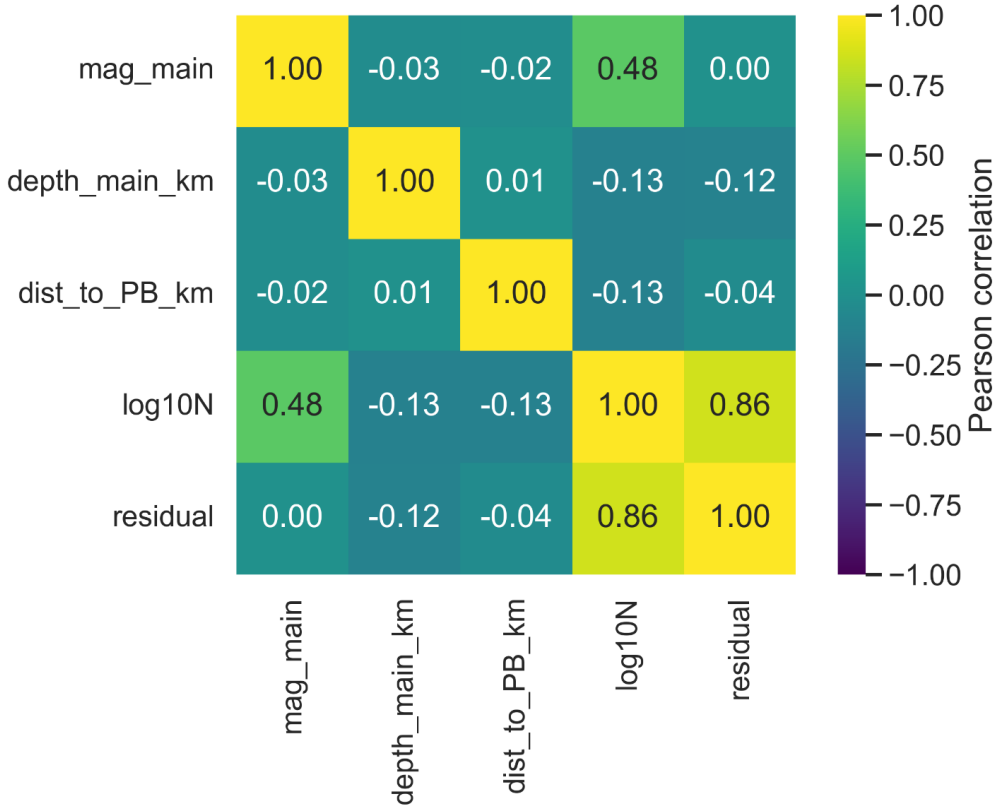

Figure 12. *Pearson correlation matrix for key variables. Correlation coefficients among Mw, depth, distance to plate boundary, $\log_{10}(N + 1)$, and regression residuals reveal a strong Mw–productivity correlation and only weak associations with depth and distance, confirming magnitude as the dominant global control.*

https://doi.org/10.5194/egusphere-2026-877
Preprint. Discussion started: 22 June 2026

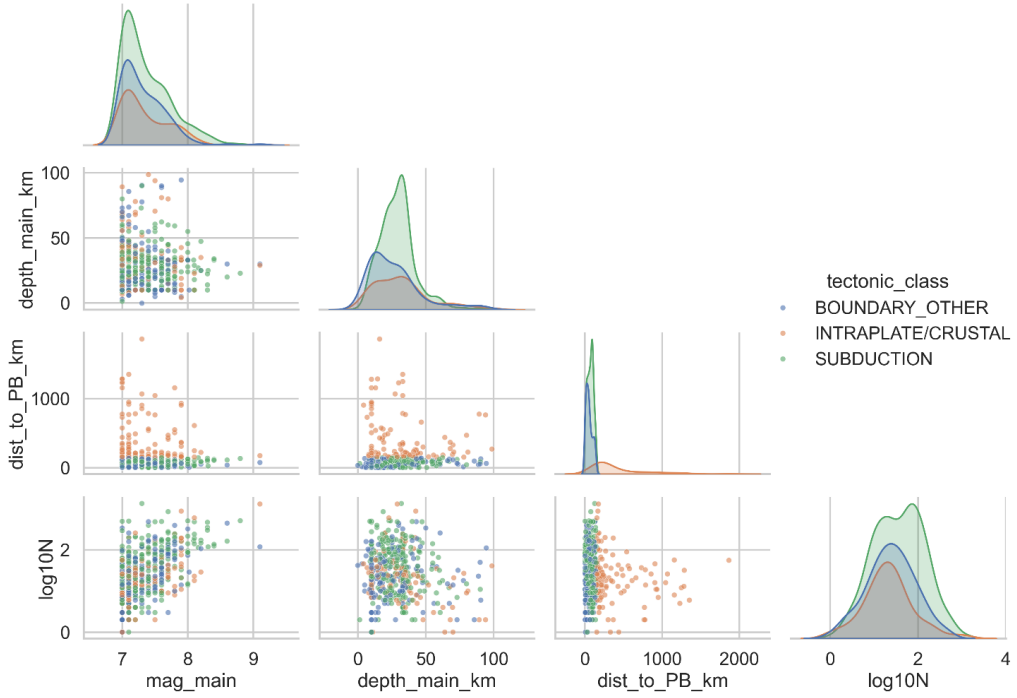

Figure 13. *Pairwise distribution of mainshock and aftershock sequence parameters. Joint and marginal distributions of Mw, depth, distance, and $\log_{10}(N + 1)$, color-coded by tectonic setting. The plots illustrate clustering of boundary events near plate interfaces, distinct depth ranges, and consistent magnitude–productivity scaling across classes.*

https://doi.org/10.5194/egusphere-2026-877
Preprint. Discussion started: 22 June 2026

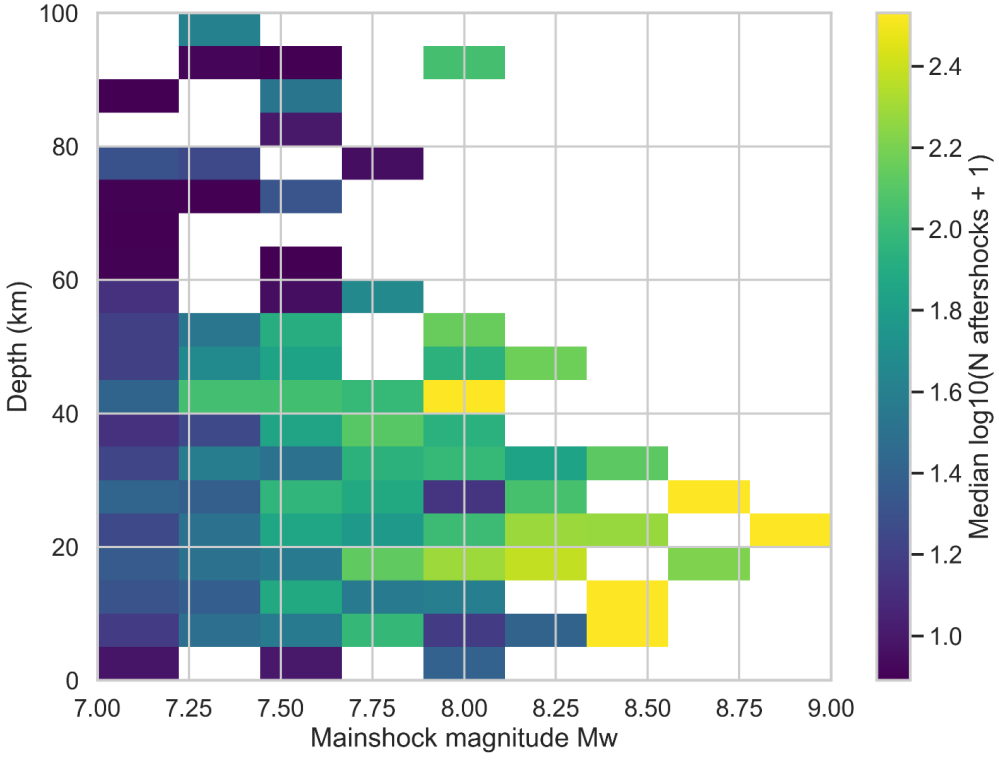

Figure 14. *Mw–depth heatmap of median aftershock productivity. Productivity ($\log_{10}(N + 1)$) is averaged within bins of mainshock magnitude and focal depth. Higher productivity occurs for shallow, large-magnitude earthquakes. White bins indicate sparse or absent data.*

https://doi.org/10.5194/egusphere-2026-877
Preprint. Discussion started: 22 June 2026

Table 1. *OLS regression parameters for the magnitude–productivity scaling $\log_{10}(N + 1) = a + bMw$. Reported values include intercept a, slope b, standard errors, confidence intervals, R^2, and number of sequences in each tectonic class.*

Tectonic class	n	a (intercept)	SE(a)	b (slope)	SE(b)	R^2
SUBDUCTION	260	-4.0533	0.6388	0.7626	0.0867	0.2308
BOUNDARY_OTHER	160	-4.5423	0.8508	0.8097	0.1161	0.2354
INTRAPLATE/CRUSTAL	112	-4.3458	0.9196	0.7707	0.1249	0.2572

https://doi.org/10.5194/egusphere-2026-877
Preprint. Discussion started: 22 June 2026

Table 2. *Statistical comparison of aftershock productivity across tectonic settings. Results include one-way ANOVA on $\log_{10}(N + 1)$, Kruskal–Wallis test, and effect sizes, demonstrating significant differences among the three classes.*

Test	Statistic	p-value	Significance	Notes
ANOVA (log10(N+1))	F = 8.686	0.000194	Significant	Subduction differs
Kruskal–Wallis (log10(N+1))	H = 16.866	0.000218	Significant	Consistent with ANOVA
ANOVA (residuals)	F = 0.000058	0.99994	Not significant	No residual differences
Kruskal–Wallis (residuals)	H = 0.046	0.9771	Not significant	Consistent with ANOVA

https://doi.org/10.5194/egusphere-2026-877
Preprint. Discussion started: 22 June 2026

Table 3. *Post-hoc comparisons among tectonic settings. Tukey HSD (parametric) and Dunn's test with Holm correction (non-parametric) quantify pairwise differences in aftershock productivity between subduction, boundary, and intraplate earthquakes.*

Comparison	Method	p-value	Significance
SUBDUCTION vs BOUNDARY_OTHER	Tukey HSD	0.0066	Significant
SUBDUCTION vs INTRAPLATE/CRUSTAL	Tukey HSD	0.0007	Significant
BOUNDARY_OTHER vs INTRAPLATE/CRUSTAL	Tukey HSD	0.6418	Not significant
SUBDUCTION vs BOUNDARY_OTHER	Dunn Holm	0.0091	Significant
SUBDUCTION vs INTRAPLATE/CRUSTAL	Dunn Holm	0.00052	Significant
BOUNDARY_OTHER vs INTRAPLATE/CRUSTAL	Dunn Holm	0.25835	Not significant